

Eckels, S.J. and B.A. Tesene, *A comparison of R-22, R-134a, R-410a, and R-407c condensation performance in smooth and enhanced tubes: part 1, heat transfer*. ASHRAE Transactions, 1999. **105**(2): p. 428-441.

A COMPARISON OF R-22, R-134A, R-410A AND R-407C CONDENSATION PERFORMANCE IN SMOOTH AND ENHANCED TUBES: PART I, HEAT TRANSFER

S.J. Eckels
Member, ASHRAE

B. Tesene
Student

ABSTRACT

Local and average heat transfer coefficients during condensation are reported for R-22, R-134a, R-410a, and R-407c in one smooth tube and three enhanced surface tubes. The test tubes included a 3/8 inch (9.52 mm) outer diameter smooth tube, a 3/8 inch (9.52 mm) outer diameter micro-fin tube, a 5/16 inch (7.94 mm) outer diameter micro-fin tube, and a 5/8 inch (15.88 mm) outer diameter micro-fin tube. The local and average heat transfer coefficients were measured over a mass flux range of 92,100 lb/ft² hr (125 kg/m² s) to 442,200 lb/ft² hr (600 kg/m² s), and at saturation temperatures of 104 F (40 C) and 122 F (50 C).

A comparison of the performance of the different refrigerants reveals that R-134a has the highest heat transfer performance followed by R-22 and R-410a which have similar performances. In general, R-407c had the lowest performance of the refrigerants tested. The micro-fin tube more than doubles the heat transfer coefficient compared to the smooth tube for all refrigerants at the low mass fluxes, but only increases the heat transfer coefficients by 50% at the highest mass flux tested. The measured heat transfer coefficients are also compared with a number of correlations for condensation.

Introduction

This paper reports on the condensation heat transfer performance of refrigerants being considered as possible replacements for R-22. Specifically, refrigerants R-410a, R-407c and R-134a were investigated, in addition to R-22. R-410a is a higher pressure refrigerant that is a near-azeotropic mixture of R-32 and R-125 (50%/50% by mass). R-407c is a zeotropic mixture of R-32, R-125, and R-134a (23%/25%/52% by mass). The operating pressure for R-407c is similar to that of R-22, but it has a temperature glide of about 6 C (10 F) at typical condenser pressures. The study determined heat transfer coefficients and pressure drops during condensation of these refrigerants in four test tubes. The heat transfer results are presented in Part I and the pressure drop results in Part II.

Local and average heat transfer coefficients for the four refrigerants are reported in four test tubes, at two different saturation temperatures, over a range of mass fluxes, and over a range of thermodynamic qualities. The test tubes included a 3/8 inch (9.52 mm) outer diameter smooth tube, a 3/8 inch (9.52 mm) outer diameter micro-fin tube, a 5/16 inch (7.94 mm) outer diameter micro-fin tube, and a 5/8 inch (15.88 mm) outer diameter micro-fin tube. All enhanced tubes were helical rib micro-fin tubes. The quality dependence for condensation heat transfer coefficients was determined by measuring local heat transfer coefficients along the length of the test tubes. The special instrumentation required for measuring local heat transfer coefficients was only installed in the 3/8 inch (9.52 mm) outer diameter tubes, but average heat transfer coefficients are determined in all tubes.

The first section reviews previous work documenting heat transfer coefficients during condensation of alternate refrigerants and refrigerant mixtures. The next section discusses the test sections and the experimental facility used to obtain the data. Data analysis procedures and experimental uncertainties are also presented for both local and average heat transfer coefficients. The final section presents and discusses the experimental results of this study.

Literature Review

Studies on condensation of refrigerant mixtures indicated that the mixtures tend to have lower heat transfer coefficients than would be expected from a perfect mixture. For example, Stoecker and Kornota (1985) studied zeotropic R-12/R-114 mixtures condensing in a 0.512 inch (13mm) horizontal glass tube. They reported reductions in the heat transfer coefficients for zeotropic mixtures but also found that this reduction was dependent on flow pattern. Tandon et al. (1986) also measured semi-local heat transfer coefficients in a 0.394 inch (10mm) tube using a mixture of R-22 and R-12. They found that the mixture heat transfer coefficients fell between those of R-12 and R-22, but that the dependence on the mixture composition was very complicated. Mochizuki et al. (1988) showed that the effect of mixture composition on heat transfer performance was dependent on Reynolds numbers. They found that the resulting heat transfer coefficients fell between those of R-11 and R-113, and that, at high Reynolds numbers, the heat transfer performance of the mixture was not necessarily inferior to that of the pure components. Finally, Gayet et al. (1992) measured local heat transfer coefficients for a R-22/R-114 mixture in a 0.63 inch (16 mm) tube. Measured heat transfer coefficients were compared to those for the pure components as well as to a correlation published by Bell and Ghaly (1972). Bell and Ghaly correlation generally over-predicted the measured heat transfer coefficients but showed agreement within $\pm 25\%$ in all cases. This series of studies on refrigerant mixtures indicate that mixtures tend to degrade the refrigerant performance but that this is dependent on the temperature glide and mass flux of interest. Increased temperature glide increases the sensible energy transfer required to complete condensation and increases the potential for mass transfer resistance which usually results in decreased performance. As the mass flux and flow pattern change the mass transfer resistance will also change as indicated in a number of studies.

A number of studies have also reported results for refrigerant mixtures of interest in this study. For example, Doerr et al. (1994) reports heat transfer coefficients and pressure drops for five zeotropic refrigerant mixtures and pure R-125 in a smooth 3/8 inch (9.52 mm) outer diameter copper tube. The mixtures tested were by mass: R-125(40%)/R-32(60%), R-134a(90%)/R-32(10%), R-134a(75%)/R-32(25%), R-32(30%)/R-125(10%)/R-134a(60%), and R-125(44%)/R-134a(53%)/R-134a(4%). All results were compared against baseline data for R-22. They reported that the R-32(60%)/R-125(40%) mixture had a heat transfer coefficient higher than that of R-22 when compared on an equal mass flux basis and performed better than all of the other mixtures tested.

Ro et al. (1994) measured semi-local heat transfer coefficients in the condenser of a heat pump system using pure R-22 and a 30/70 mixture of R-32 and R-134a. When compared on the basis of similar heating capacity rather than mass flux, the average heat transfer coefficients for the R-32/R-134a mixture were found to be 10 to 20% lower than those for R-22.

Wijaya and Spatz (1995) measured average heat transfer coefficients for R-410a and pure R-22. Tests were conducted in a 10 ft (3.05 m) long, 0.305 inch (7.75 mm) diameter tube. They expected the mixture to perform slightly better than pure R-22 based on its thermal properties. By comparing the semi-local heat transfer coefficients, they found that, over the

entire range, the mixture performed 2 to 6% better than R-22. Chitti and Anand (1996) compared also compared the performance of R-22 and R-410a in a 3/8 inch (8.0 mm) smooth tube. They found that R-410a had higher heat transfer coefficients at higher mass fluxes, but also found that R-22 had significantly higher heat transfer coefficients at the lower mass fluxes. They attributed some of the difference to the high experimental uncertainty at the lower mass fluxes.

Dobson and Chato (1998) compared the performance of R-22, R-410a, and R-134a in a 0.276 inch (7.04 mm) diameter smooth tube. The performance of the three refrigerants was similar in the wavy flow regime, while in the annular flow regime R-134a had the highest heat transfer coefficients. Kedzierski and Goncalves (1997) compared the performance of R-134a, R-410a, R-125 and R-32 in a 3/8 inch (9.52 mm) micro-fin tube. When compared at a mass flux of 184,000 lb/hr ft² (250 kg/m² s), the R-410a and R-134a had nearly identical performance. Dunn (1996) compared the heat transfer performance of six R-22 replacements and four R-502 replacement in a 3/8 inch (9.52 mm) micro-fin tube. For the R-22 group, they found that R-134a had the highest performance by about 10%, while R-22 and R-410a had similar performance, and R-407c had the lowest performance.

Experimental Facility

The experimental facility used in this study was designed specifically for measuring condensation heat transfer coefficients. The facility contains five main systems: the test sections, the refrigerant loop, the annulus loop, the boiler loop, and the data acquisition system. A schematic diagram of the test facility is shown in Figure 1. The main feature of this system is the pump driven refrigerant loop. The test tubes are mounted in a tube-in-tube counter flow heat exchanger with the cooling fluid supplied by the annulus loop. The boiler loop supplies energy for vaporization of the refrigerant prior to entering the test section. The following sections summarize each of these main systems.

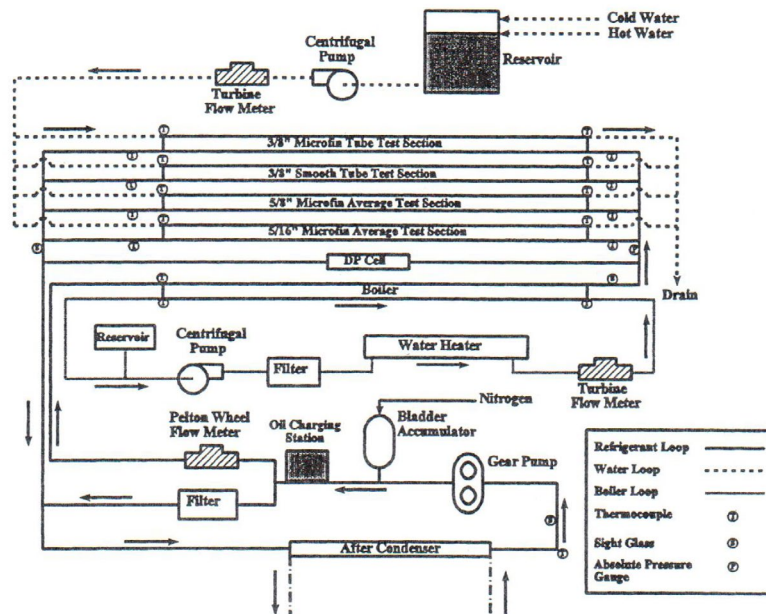


Figure 1: Schematic of test facility

Test Section

The test facility has four active test sections. The 3/8 inch (9.52 mm) outer diameter smooth and micro-fin tubes are mounted in test sections with instrumentation to measure average and local heat transfer coefficients. The remaining two test sections utilize 5/16 inch (7.92 mm) and 5/8 inch (15.88 mm) outer diameter micro-fin tubes and are only instrumented to measure average heat transfer coefficients. The dimensions of the test sections and test tubes are summarized in Table #1. Cooling water flows in the annulus and refrigerant flows in-tube. A series of valves route the refrigerant to the desired test section.

Table 1: Test Section Dimensions

	3/8" Smooth Tube	3/8" Microfin Tube	5/8" Microfin Tube	5/16" Microfin Tube
Inner tube od, inch (mm)	3/8 (9.53)	3/8 (9.53)	5/8 (15.88)	5/16 (7.94)
Inner tube id, inch (mm)	0.315 (8.01)	0.351 (8.92)	0.575 (14.61)	0.289 (7.34)
Outer tube id, inch (mm)	0.666 (16.91)	0.666 (16.91)	0.785 (19.94)	0.545 (13.84)
Overall Length, ft (m)	10 (3.048)	10.3 (3.148)	10.3 (3.148)	10.3 (3.148)
Ridge Count	N/A	60	60	50
Helix Angle (deg.)	N/A	18	27	18
Included Angle	N/A	51	45	57
Fin Height, inch (mm)	N/A	0.008 (0.203)	0.012 (0.305)	0.008 (0.203)
Distance Between Pressure Taps, ft (m)	12.5 (3.810)	12.4 (3.780)	12.5 (3.810)	12.4 (3.780)

The temperature of the refrigerant and the annulus fluid are measured at the inlet and outlet of the 3/8 inch (9.52 mm) smooth and micro-fin tube test sections with type-T thermocouples. Type-T thermocouples also measure the temperature of the annulus fluid at regularly spaced intervals along the length of the test section. This information is used to determine the local heat flux along the tube length. The thermocouples in the annulus gap are a bead type, inserted into the fluid stream through holes tapped in the top and bottom of the annulus tube. Specifically, the thermocouple bead mounts in the end of a small piece of copper tubing which is threaded at one end. The thermocouple bead mounts slightly extended from the end of the small copper tube and is held in place with epoxy. The copper tubing screws into the tapped holes in the annulus wall so that the bead is positioned at the midpoint of the annulus gap. The annulus thermocouples are placed at one foot intervals along the length of the test tube, except at the inlet and outlet where a 6 inch spacing was used.

The average test sections utilize 5/16 inch (7.92 mm) and 5/8 inch (15.88 mm) micro-fin tubes in a counter flow tube-in-tube heat exchanger design. Table 1 lists the dimensions of these test sections. Type-T thermocouples measure the inlet and outlet water and refrigerant temperatures. The average test sections are not instrumented to determine local annulus fluid temperatures.

A 0 to 500 pisa (0 to 3.447 MPa) absolute pressure transducer, with a resolution of ± 0.5 psi (3.45 kPa), records the pressure at the inlet of the test sections. A 0 to 20 psid (0 to 138 kPa) differential pressure transducer having a resolution of ± 0.02 psi (132 Pa) measures the pressure drop of the refrigerant flowing through the test sections. All thermocouples in the test section have been calibrated to within ± 0.27 F (± 0.15 C).

Refrigerant Loop

The refrigerant loop supplies refrigerant to the test sections at a known flow rate and quality. The loop consists of an after-condenser, a pump, an accumulator-bladder, a refrigerant

flow meter, and a boiler, which are shown in Figure 1. The refrigerant exiting the test section condenses and is sub-cooled in the after-condenser. The after-condenser is a tube-in-tube heat exchanger which helps to minimize fractionation effects with refrigerant blends. A positive displacement gear pump located at the outlet of the after condenser circulates the refrigerant. The accumulator-bladder located on the high side of the gear pump performs the following functions: it acts as a dampening device for the system and provides a variable volume reservoir for the system. Adjusting the amount of liquid refrigerant contained in the accumulator regulates system pressure. A by-pass line controls the flow of refrigerant to the test section. A flow meter with a resolution of $\pm 1\%$ measures the refrigerant flow rate prior to entering the boiler.

Annulus Loop

The annulus loop supplies the cooling medium to the test sections. The loop contains a reservoir, a pump, a heater, and a flow meter. The temperature difference between the refrigerant in the test section and the annulus fluid determines to a large degree the quality change of the refrigerant in the test section. Mixing hot and cold tap water into a 50 gallon (190 L) reservoir sets the gross temperature of the annulus fluid. An immersion heater located upstream of the pump is an additional control used to set the final water temperature. A centrifugal pump circulates the fluid from the tank to the test sections. A turbine flow meter with an accuracy of $\pm 1\%$ measures the flow rate.

Boiler Loop

The boiler loop supplies energy for vaporization of the refrigerant. The loop contains a pump, an expansion tank, immersion heaters, a flow meter, and the boiler in the refrigerant loop. A centrifugal pump circulates the water through the loop and an angle valve provides flow control. Three 15,350 Btu/hr (4.5 kW) immersion heaters controlled with rheostats supply energy to the circulating water. A turbine flow meter accurate to $\pm 1\%$ measures the boiler water flow rate. Type-T thermocouples calibrated to ± 0.27 F (± 0.15 C) measure the fluid temperature at the inlet and outlet of the boiler.

Data Acquisition System

The data acquisition system uses a computer card designed specifically for reading thermocouple and voltage inputs. The system monitors all thermocouple inputs and the voltage readings from flow meters and pressure transducers. A program written in C is used to observe the system parameters during initial startup. Once the system parameters have come to a steady reading, the system is allowed to circulate for about 15 minutes. If no additional changes are detected, the final data acquisition is started. Final data acquisition scans each channel 50 times, which requires about five minutes. The final data analysis uses the average reading from each channel.

Data Analysis

The following sections present data analysis equations for both local and average heat transfer coefficients. Local heat transfer coefficients are determined in the 3/8 inch (9.52 mm) smooth and micro-fin tube. Average heat transfer coefficients are determined in all four test tubes. The first two sections review the equations for determining the local and average heat transfer coefficients. The methods used for determining refrigerant properties for pure

refrigerants and refrigerant mixtures are also discussed. The final section presents experimental uncertainties for the local and average heat transfer coefficients.

Local Heat Transfer Coefficients

Type-T thermocouples placed in the annulus gap measure the axial temperature profile in the annulus fluid. At each annulus station, the top and bottom thermocouples are averaged and this fluid temperature is fit to a two degree polynomial as a function of axial position:

$$T = f(z) \quad (1)$$

The local variation in heat flux along the length of the tube can be related to the derivative of the temperature profile with an energy balance, yielding the following equation for local heat flux:

$$q'(z) = \frac{m \cdot c_p \cdot \frac{dT}{dz}}{\pi \cdot D_o} \quad (2)$$

The next step in determining the local heat transfer coefficients is to draw the thermal resistance network, from the measured annulus temperature to the inner refrigerant temperature expressed in terms of the total heat transfer:

$$q(z) = \frac{T_r - T_a}{\frac{1}{h_i \cdot A_i} + \frac{\ln(D_o/D_i)}{2 \cdot \pi \cdot k \cdot L} + \frac{1}{h_a \cdot A_a}} \quad (3)$$

The inner refrigerant temperature (T_r) is inferred from the pressure reading and is not directly measured. The method for calculating refrigerant saturation temperature is discussed further in a following section. Rearranging the equation in terms of the outer surface heat flux yields:

$$q'(z) = \frac{T_r - T_a}{\frac{D_o}{h_i \cdot D_i} + \frac{D_o \cdot \ln(D_o/D_i)}{2 \cdot k} + \frac{1}{h_a}} \quad (4)$$

Equations 2 and 4 can now be solved for the heat transfer coefficient on the inner surface:

$$h_i = \frac{1}{\frac{(T_r - T_a) \cdot \pi \cdot D_i}{m \cdot c_p \cdot \frac{dT}{dz}} - \frac{D_i}{h_a \cdot D_o} - \frac{D_i \cdot \ln(D_o/D_i)}{2 \cdot k}} \quad (5)$$

Five local heat transfer coefficients are determined along the length of the tube during each data run. Measuring the local heat transfer coefficient requires finding the temperature distribution in the annulus fluid and the heat transfer coefficient on the annulus side of the heat exchanger. A modified Wilson plot technique (Briggs and Young 1969) provided a correlation for the annulus side heat transfer coefficient. The inner tube diameter used in Equation 5 is the root diameter of the test tube, which is defined as the outer diameter of the tube minus the wall thickness. For the micro-fin tube, this means the additional surface area added by the fins is lumped into the heat transfer coefficient. Application of the resulting heat transfer coefficients also requires that the root diameter be used in surface area calculations.

The refrigerant qualities can be calculated by applying a series of energy balances to the boiler and test sections. The outlet quality for the boiler is determined from an energy balance

on water and refrigerant streams. The energy transfer to the refrigerant in the boiler is found from the known water mass flow rate and temperature difference:

$$q_b = \dot{m} \cdot c_{p,w} \cdot (T_{w,i} - T_{w,o}) \quad (6)$$

A similar expression is found for the refrigerant stream from the enthalpy change of the refrigerant across the boiler:

$$q_b = \dot{m}_r \cdot i_{fg} \cdot x + \dot{m}_r \cdot c_{pr} \cdot (T_{sat} - T_{r,i}) \quad (7)$$

Equations 6 and 7 can then be solved for the outlet quality. The outlet quality for the boiler is also the inlet quality for the test section. The energy transfer in the test section is

$$q_a = \dot{m}_w \cdot c_{pw} \cdot (T_{w,i} - T_{w,o}) \quad (8)$$

Since the refrigerant in the test section is two-phase, the expression for refrigerant enthalpy difference from inlet to outlet reduces to

$$q_a = \dot{m}_r \cdot i_{fg} \cdot \Delta x \quad (9)$$

The quality change across the test section is also found by equating Equations 8 and 9. The local qualities along the length of the test section are found by using the outlet water temperature and the local annulus fluid temperatures in Equation 8.

Average Heat Transfer Coefficients

The average inner-tube heat transfer coefficients are found from the overall heat transfer coefficient and the annulus side heat transfer coefficient. The overall heat transfer coefficient is calculated from

$$U_a = \frac{q_a}{A_a \cdot \Delta T_{lm}} \quad (10)$$

The test section heat transfer (q_a) is found from the annulus fluid flow rate and temperature difference (Equation 10). The log-mean-temperature-difference is based on the water inlet and outlet temperatures and the inlet and outlet saturation temperatures of the refrigerant. Calculation of saturation temperature is discussed further in the next section. Expressing the overall heat transfer coefficients as a sum of resistances and solving for the in-tube heat transfer coefficient, assuming that the resistance of the copper tube is negligible, yields:

$$h_r = \frac{1}{\left(\frac{1}{U_a} - \frac{1}{h_a}\right) \cdot \frac{A_r}{A_a}} \quad (11)$$

The surface area used in Equation 11 is based on the root diameter of the test tubes.

Refrigerant Properties

The data analysis equations outlined above for determining local and average heat transfer coefficients apply for either pure refrigerants or refrigerant mixtures. The only difference in the analysis of refrigerant mixtures is the method used to determine the saturation temperature. For the local heat transfer coefficients, the local refrigerant temperature must be calculated, while for the average heat transfer coefficient, the inlet and outlet saturation temperature must be determined. The saturation temperature for the pure refrigerant used in

Equation 10 to calculate the log-mean-temperature-difference is inferred from the pressure readings at the inlet and outlet of the test section which are known from the pressure transducer and differential pressure transducer. The saturation temperature used in Equation 5, for pure refrigerants, is calculated assuming a linear variation in pressure drop over the test section. For refrigerant mixtures, the pressure and enthalpy of the refrigerant sets the two-phase temperature via a condensation curve. This study investigated two refrigerant mixtures: R-410a and R-407c. Due to the low temperature glide of R-410a, the condensation curve was assumed to be linear from bubble point to dew point. The saturation temperatures used in Equations 5 and 10 were determined from the dew point and bubble point evaluated at the average pressure in the test section assuming the variation was linear with quality. For R-407c, condensation curves were generated for each data run with the method outline by Thome et al (1997), at the average pressure in the test section. The method outlined by Thome et al (1997) was used to generate the condensation curves because it most closely predicted the measured inlet and outlet temperatures with R-407c.

Experimental Uncertainties

The experimental uncertainties in the average and local heat transfer coefficients reported in this paper were estimated with a propagation-of-error analysis (Kline and Mcklintock 1953). As a reference, uncertainties were calculated for R-22 data runs. Propagation-of-error when applied to Equation 5 estimates the uncertainty in the local heat transfer coefficients. Applying the propagation-of-error method to Equation 5 requires determining the uncertainty in the annulus temperature slope (dT/dz). A second order polynomial was fitted to the annulus temperature profiles, and then the derivative of this equation yields the desired slopes. The uncertainty in the slope was estimated using a simple linear ($\Delta T/\Delta z$). The test matrix for local data used two quality ranges. The first series of tests had a quality change of 80% to 90% over the test section, while the second series had a quality change of about 40% over the test section. Table 2 presents experimental uncertainty in the local heat transfer coefficient at each of the 5 local stations for the large load (large quality change) and low load (low quality change) cases. Table 2 shows that the local heat transfer coefficients at the lower loads have considerably larger uncertainty than those at the larger loads. In the micro-fin tube, the uncertainty at the first station can be as large as $\pm 80\%$ at the lowest mass flux and as low as $\pm 10\%$ for other points. For the smooth tube, the uncertainty in the local heat transfer coefficients ranges from $\pm 30\%$ to as low as $\pm 10\%$. The uncertainties in the R-410a and R-134a data will be similar to those listed above for R-22. The uncertainties in the local heat transfer coefficients for R-407c will be larger than those for the other refrigerants because of the additional uncertainty associated with using the condensation curve.

Table 2: Uncertainty in local heat transfer coefficients for R-22 at high and low loads

Mass Flux lb/(hr ft ²)	Smooth Tube each station (\pm %)					Micro-Fin Tube each station (\pm %)				
	#1	#2	#3	#4	#5	#1	#2	#3	#4	#5
92,100 (High Load)	21	14	14	16	28	37	20	16	15	21
92,100 (Low Load)	30	17	15	13	19	88	42	35	26	32
184,250 (High Load)	13	8	8	7	11	22	13	11	10	15
184,250 (Low Load)	22	14	12	12	17	33	19	16	14	19
294,800 (High Load)	12	7	7	7	11	18	11	10	9	12
294,800 (Low Load)	17	11	10	9	11	33	20	17	14	20
442,200 (High Load)	11	7	7	6	9	14	9	8	8	12

442,200 (Low Load)	16	10	10	9	13	19	12	11	10	12
--------------------	----	----	----	---	----	----	----	----	----	----

Applying propagation-of-error analysis to Equation 11 estimates the uncertainty in the average heat transfer coefficients. The results show that uncertainty ranges from $\pm 6\%$ at the high mass flux to $\pm 14\%$ at low mass flux in the smooth tube, and from $\pm 8\%$ to $\pm 18\%$ in the micro-fin tube.

Experimental Results

This section presents heat transfer coefficients during condensation for R-22, R-410a, R-407c, and R-134a in the smooth tube and three micro-fin tubes. Table 1 lists the dimensions of the four test tubes. Also of interest in the micro-fin tubes is the profile of the fin used on the surface, which is shown in Figure 2 for the 3/8 inch (9.52 mm) outer diameter tube. The fins have a triangular profile with a rounded tip. The fins on the surface of the 5/16 inch (7.94 mm) and 5/8 inch (15.88 mm) micro-fin tubes have fins with similar tip profiles.

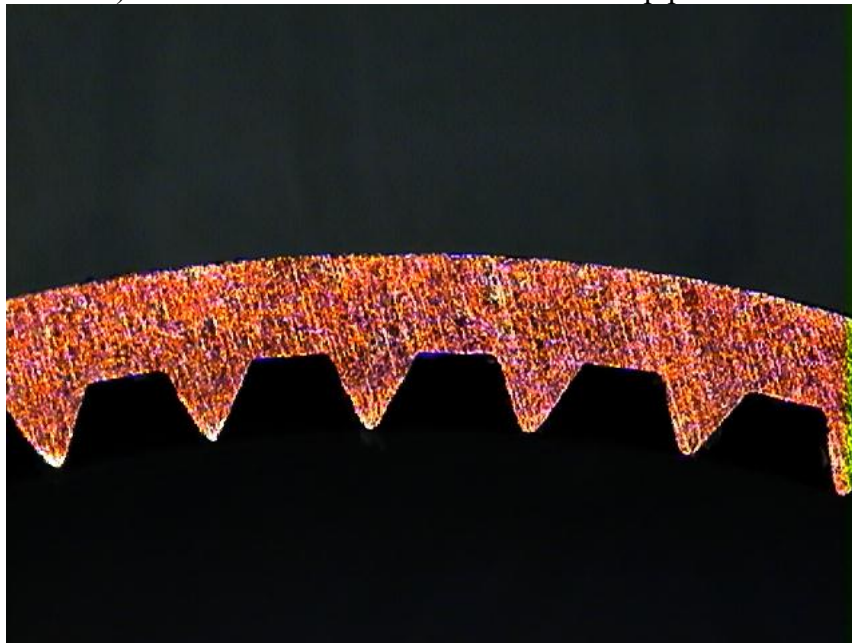


Figure 2 Profile of the fin used on the surface for the 3/8 inch (9.52 mm) outer diameter tube.

Local and average heat transfer coefficients were measured over a mass flux range of 92,100 lb/ft²hr (125 kg/m²s) to 442,200 lb/ft² hr (600 kg/m² s). An average saturation temperature of 104 F (40 °C) was tested in all tubes, while an additional saturation temperature of 122 F (50 °C) was used during local tests. For refrigerant mixtures, the average of the dew point and bubble point was approximately 104 F (40 °C) and 122 F (50 °C). The first section compares the average heat transfer coefficients for the four refrigerants tested. The second section looks at the local heat transfer coefficients for a range of qualities, mass fluxes and temperatures.

Average Heat Transfer Coefficients

Figure 3 shows the average heat transfer coefficients during condensation in the 3/8 inch (9.52 mm) outer diameter smooth and micro-fin tubes for the four refrigerants tested. The average data were taken with an inlet quality of 85% to 95% and an outlet quality of 5% to 10%. The lines shown on the figure are a second degree polynomial, least squares fit to the

experimental data. As an indication of the uncertainty, error bars have been added to the R-22 data. Figure 3 indicates that the heat transfer coefficients for the micro-fin tube are significantly higher than those for the smooth tube for all refrigerants tested. In addition, the figure shows that R-134a has the highest heat transfer coefficients in both the smooth tube and micro-fin tube, while R-407c has the lowest performance in both tubes. The performances of R-410a and R-22 are about equivalent.

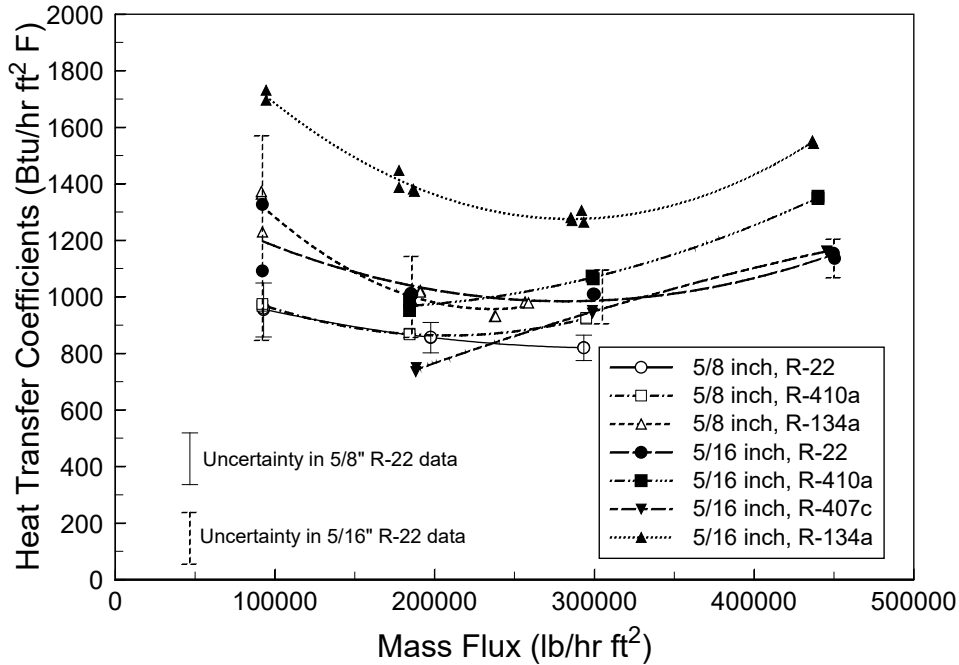


Figure 3: Average heat transfer coefficients during condensation in the 3/8 inch (9.52 mm) outer diameter smooth and micro-fin tubes for the four refrigerants tested

Figure 4 presents the average heat transfer coefficients for the 5/16 inch (7.92 mm) and 5/8 inch (15.88 mm) micro-fin tubes versus mass flux. The heat transfer coefficients for R-134a exceed those for the other refrigerants in both the 5/16 inch (7.92 mm) and 5/8 inch (15.88 mm) tubes. R-410a and R-22 have approximately the same performance in both tubes. In general, the heat transfer coefficients for the 5/16 inch (7.92 mm) tube exceed those for the 5/8 inch (15.88 mm) tube over the range of conditions tested as might be expected. Single phase heat transfer coefficients can also be shown to increase as diameter of the tube decreases in both laminar and turbulent flow when comparisons are made on an equivalent mass flux basis. For both tubes, the heat transfer coefficients decrease at first when mass flux increases then heat transfer coefficients increase at the higher mass fluxes. The lower flow rates have a higher uncertainty (which is shown in the figure for R-22), which is a possible explanation for these trends. The complex interactions between the surface fins and fluid (and thus their enhancement of turbulence over a range of Reynolds numbers) could also be contributing to this effect.

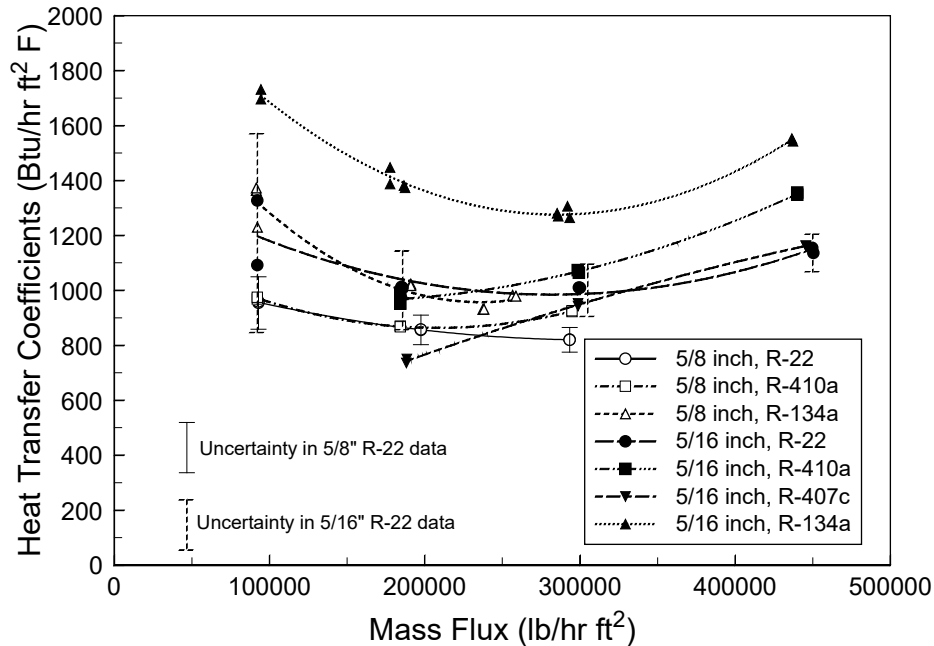


Figure 4 average heat transfer coefficients for the 5/16 inch (7.92 mm) and 5/8 inch (15.88 mm) micro-fin tubes versus mass flux

A detailed comparison of the heat transfer coefficients in the 3/8 inch (9.52 mm) micro-fin tube and the 3/8 inch (9.52 mm) smooth tube can be made by forming a ratio of the heat transfer coefficients at equivalent mass fluxes designated as the heat transfer enhancement factor (EF):

$$EF = \frac{h_{mf}}{h_{sm}} \quad (12)$$

Figure 5 shows the enhancement factor (EF) formed from the curves shown in Figure 3. The results indicate that the EF ratios for the refrigerants vary from about 2.2 to 2.5 at the lowest mass flux to about 1.2 to 1.6 at the highest mass flux. The only exception is R-407c which has a lower EF ratio at the lowest mass flux. The reason for the lower EF ratio with R-407c at the lower mass fluxes is not clear. Authors have noted that the performance of mixtures is dependent on flow rate and flow pattern (Stoecker and Kornota 1985, and Mochizuki et al 1988). It was anticipated that the micro-fin would increase turbulence and possibly aid the mixture at low flows relative to the pure refrigerants. Error bars shown on the plot for R-22 also indicate that large uncertainties exist at the low mass fluxes.

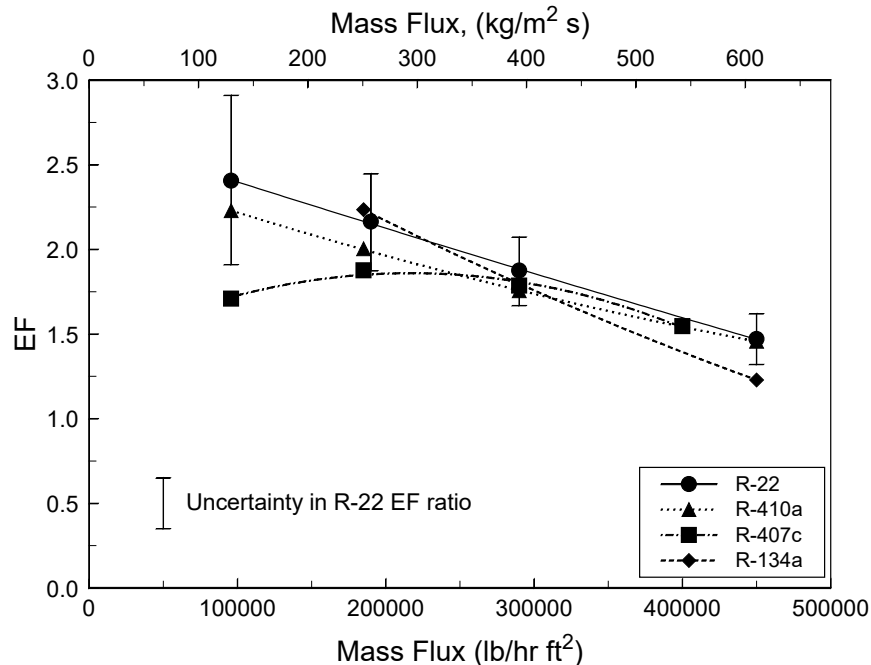


Figure 5: Enhancement factor (EF) formed from the curves shown in Figure 3.

It should also be noted that the heat transfer coefficients in the micro-fin tube are based on the nominal diameter and that the actual surface area is about 1.5 times larger than that for the smooth tube. The enhancement factor in Figure 5 is seen to run from about the area ratio at the highest mass flux to significantly higher at the lower mass fluxes. The action of the fins to enhance turbulence in the condensate layer may explain this behavior of increased benefits at lower flow rates. Another explanation is the enhancement is based on flow pattern transitions. At the lowest mass flux of 92,100 lb/ft² hr (125 kg/m²s) for R-22, the flow pattern map of Nitheanandan et al (1990) predicts that the flow in a smooth tube will transition from annular flow to wavy flow at a quality of 50%, while at the highest mass flux of 442,200 lb/ft² hr (600 kg/m² s), this transition does not occur until 18% quality. The helical rib of the micro-fin tube may be delaying the transition from annular flow to wavy flow (Manwell and Bergles 1990) which would benefit the lower flows.

Local Heat Transfer Coefficients

Local heat transfer coefficients were determined for each refrigerant at four mass fluxes and two temperatures. At each mass flux and temperature, four data runs were taken covering a range of qualities and heat loads. Figure 6 presents local heat transfer coefficients for R-22 in both the smooth tube and micro-fin tube at two mass fluxes. The lines shown on the figure are a least squares curve fit of the local data points. Figure 6 shows that the R-22 heat transfer coefficients increase with mass flux and quality. The curves appear to have some upward curvature at the higher qualities. For the micro-fin tube at the lower mass flux, the line has significant curvature at the higher qualities and even exceeds the higher mass flux line. This is likely due to the large uncertainty at the high quality and low mass flux points. To illustrate this effect, error bars have been added to the high load local points for the low mass flux curve. These bars represent the calculated uncertainty obtained in the individual points.

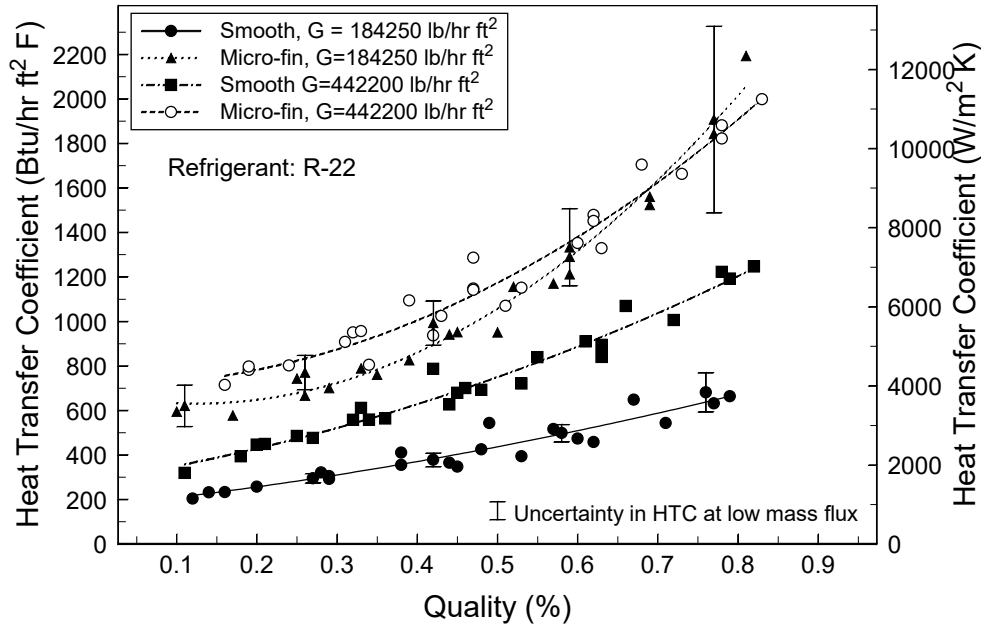


Figure 6: Local heat transfer coefficients for R-22 in both the smooth tube and microfin tube at two mass fluxes.

Figure 7 shows the effect of saturation temperature on the local condensation performance of R-22 at a mass flux of 294,800 lb/ft² hr (400 kg/m²s). The uncertainty in the large load local heat transfer coefficients are also shown in the figure. The figure indicates that the heat transfer coefficients are consistently lower with increased saturation temperature.

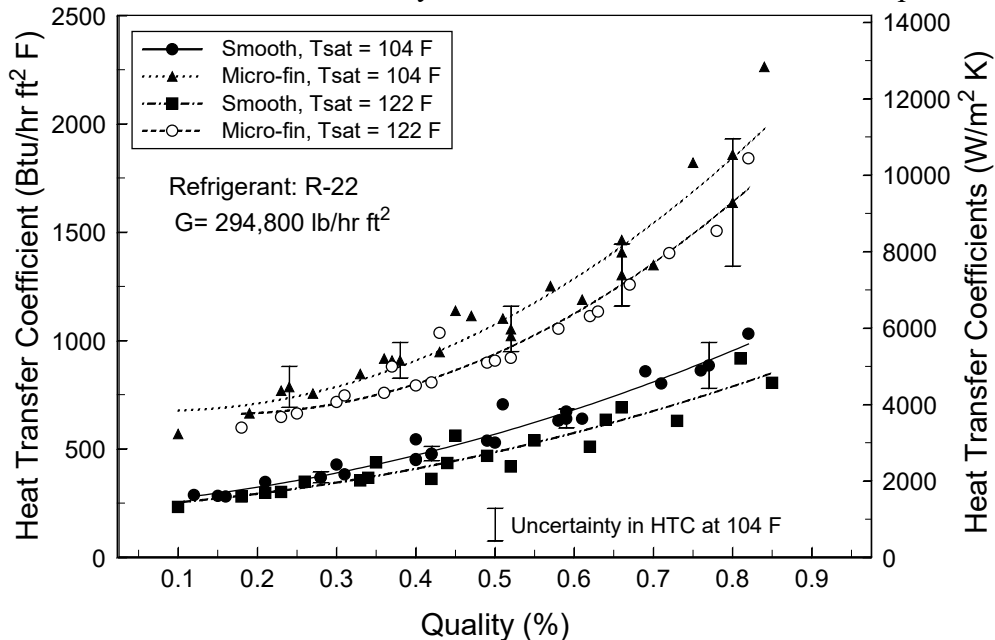


Figure 7 Effect of saturation temperature on the local condensation performance of R-22 at a mass flux of 184,250 lb/ft² hr (250 kg/m² s)

Local heat transfer coefficients for the four refrigerants are compared in Figures 8 and 9. The actual data points are not presented on the plots, only the curve-fit of the local data points

versus quality. Figure 8 presents the local heat transfer coefficients at a mass flux of 184,250 lb/ft² hr (250 kg/m² s) for the smooth and micro-fin tubes. The local curves shown for the smooth tube indicate that R-134a has the highest heat transfer coefficients over the quality range, followed by R-410a, R-22 and R-407c. At a 50% quality, the heat transfer coefficient in the smooth tube for R-134a is 1500 Btu/hr ft² F (8500 W/m² K), while for R-407c the heat transfer coefficient is 900 Btu/hr ft² F (5000 W/m² K). Figure 8 also shows that the quality dependence is similar for the four refrigerants tested. Figure 9 presents similar information for the higher mass flux of 442,200 lb/ft²hr (600 kg/m²s). The local data reveal that R-134a has the highest local heat transfer coefficients in both the smooth tube and micro-fin tube. The performance of R-410a and R-22 are almost identical for the range of conditions covered and that R-407c has the lowest performance in most cases, but the difference appears to decrease as mass flux increases.

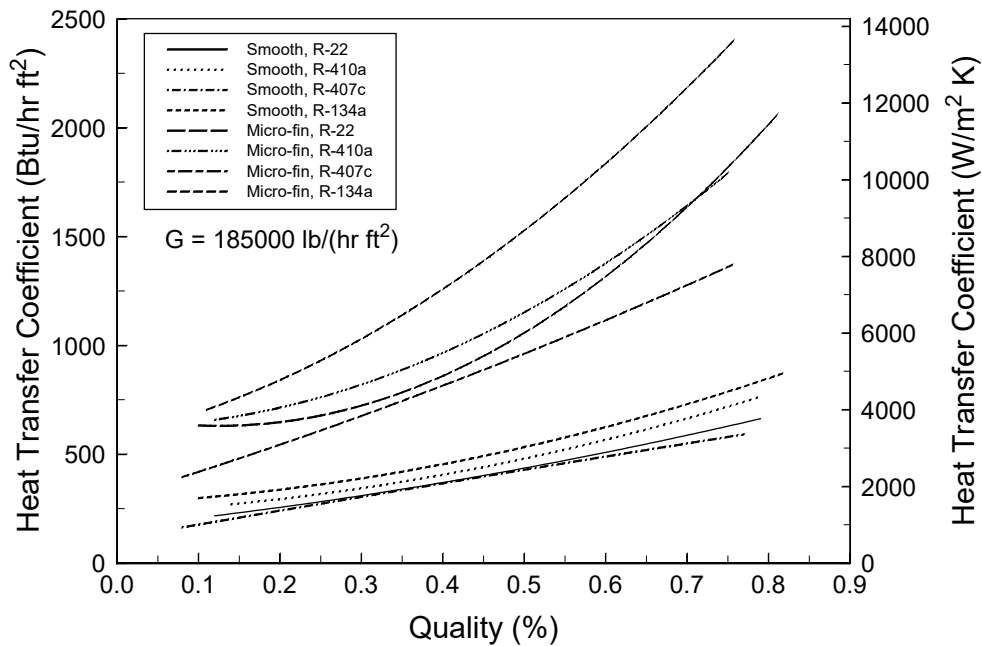


Figure 8: Local heat transfer coefficients at a mass flux of 184,250 lb/ft² hr (250 kg/m² s) for the smooth and microfin tubes.

The relative local performance of the micro-fin tube can be determined from the heat transfer enhancement factor (EF), which is formed from the local curve fits by dividing the local heat transfer coefficient in the micro-fin tube by the local heat transfer coefficient for the smooth tube at similar qualities. Figure 10 shows the local heat transfer enhancement factor for the four refrigerants at a mass flux of 442,200 lb/ft²hr (600 kg/(m² s)). The EF ratio ranges from about 1.6 at the high quality to about 2.0 at the lower quality. This figure indicates that the heat transfer enhancement due to the micro-fin tube is more pronounced at the lower quality. The transition of the flow from annular to wavy flow, which is predicted to happen at about 15-20% quality for both R-22 and R-134a by the Nitheanandan et al (1990) flow pattern map for this mass flux, may be causing this increased EF ratio at the low qualities.

It is also interesting to compare the EF ratios found from the average heat transfer coefficients with those produced from the local heat transfer coefficients. The average EF ratios from Figure 4 ranged from 1.6 to 1.3 for the highest mass flux. Noting that the quality range on the local EF curve shown in Figure 10 is smaller than that for the average point, the average of the local EF ratios appears to be slightly higher than the average EF ratio.

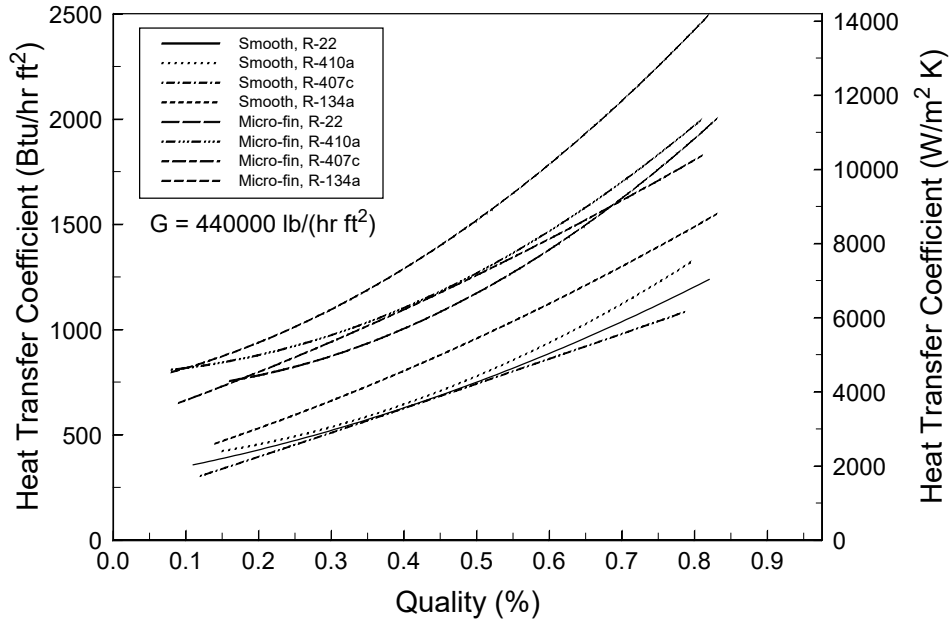


Figure 9 Local heat transfer coefficients at a mass flux of $442,200 \text{ lb/ft}^2\text{hr}$ ($600 \text{ kg/m}^2\text{s}$) for the smooth and microfin tubes

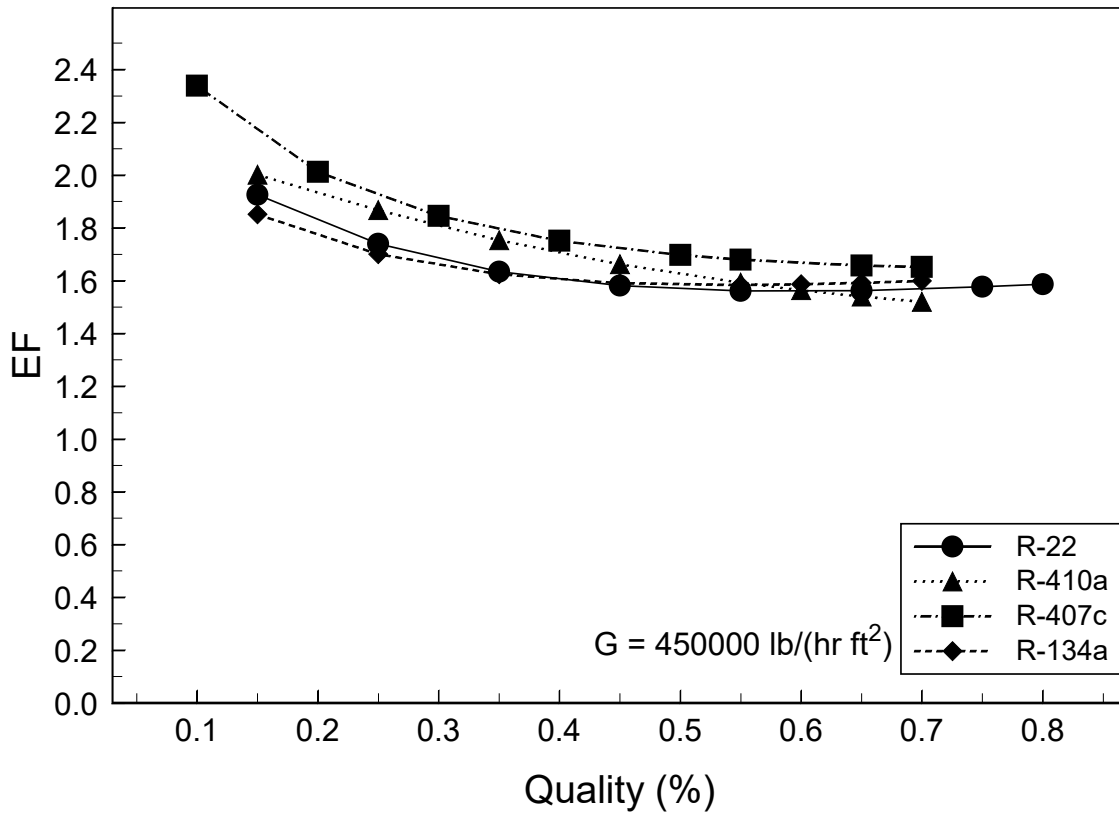


Figure 10: Local heat transfer enhancement factor for the four refrigerants at a mass flux of $442,200 \text{ lb/ft}^2\text{hr}$ ($600 \text{ kg/m}^2 \text{ s}$)

Figure 11 shows the local enhancement factor at a lower mass flux of 184,250 lb/ft²hr (250 kg/(m² s)). The EF ratios appear flatter or even increasing with increased quality. The EF ratios are all significantly higher than those of Figure 10. For the smooth tube, the flow transitions to wavy flow occurs at a quality of about 30% for a mass flux of 184,250 lb/ft²hr (250 kg/(m² s)). For the wavy flow region, the EF ratios range from 2.4 to 1.9 in Figure 10 and from 2.7 to 2.1 in Figure 11. For the annular flow region, the EF ratios ranges from 1.8 to 1.5 in Figure 10 and from 2.2 to 2.9 in Figure 11. This indicates that the higher enhancement factors at the lower mass fluxes is due to the enhancement of the annular flow region.

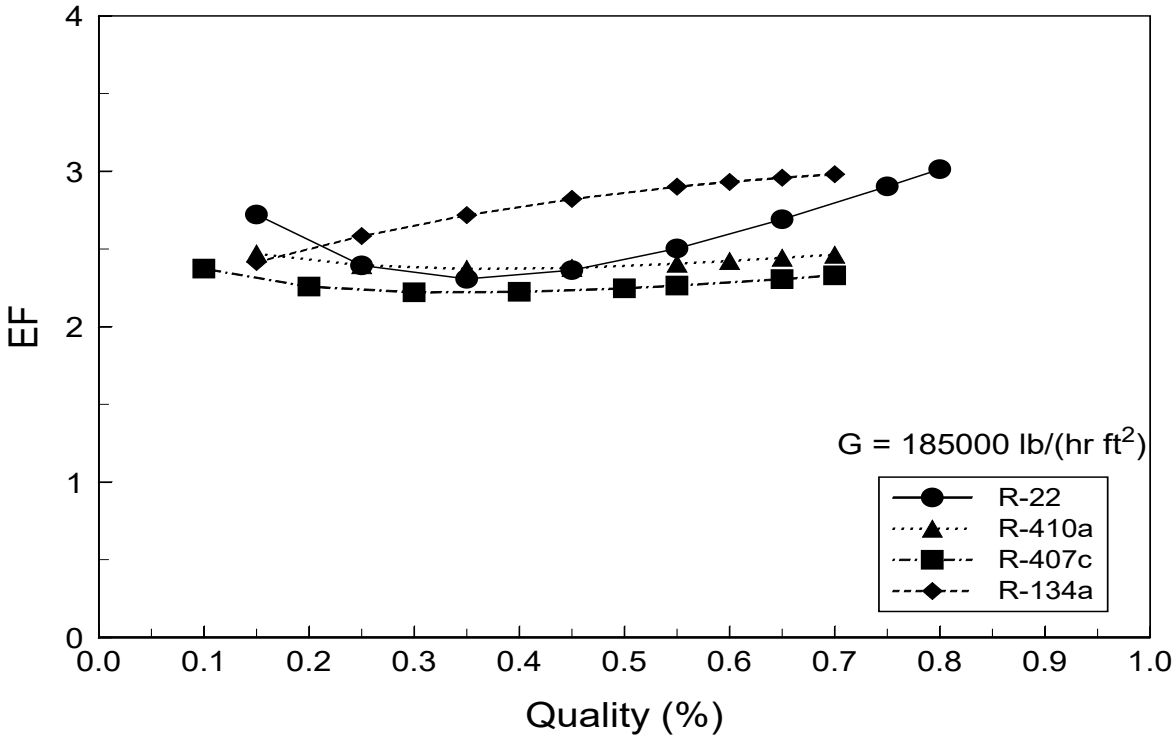


Figure 11: Local heat transfer coefficients enhancement factor for the four refrigerants at a mass flux of 184,250 lb/ft²hr (250 kg/(m² s))

Comparison with correlations

The experimental data presented in the previous sections were compared with a number of currently available correlations for in-tube condensation. The correlations selected were: Shah (1979), Cavallini and Zecchin (1974), Akers et al (1959), and Moser and Webb (1998). The correlations were compared with the smooth tube heat transfer coefficients of the four refrigerants reported in this paper. Since R-407c is nonazetropic, the correlations are not expected to accurately predict its performance but it is informative to list this comparison in addition to R-134a, R-22, and R-410a. For each data point in the data base, the percent deviation defined as:

$$\%Deviation = \frac{h_{pred} - h_{exp}}{h_{exp}} \cdot 100 \quad (13)$$

was calculated for each data point. The average of the absolute values of the percent deviations (ABSPD) is then calculated for each correlation and refrigerant combination.

$$ABSPD = \frac{\sum abs(\%Deviation)}{n} \quad (14)$$

This measure gives an indication of the average size of the deviation regardless of the positive or negative. The straight average percent deviation (APD) was also calculated for each refrigerant and correlation combination.

$$APD = \frac{\sum \%Deviation}{n} \quad (15)$$

The APD gives a general indication if the correlation is over or under predicting the heat transfer coefficients. Tables 3 and 4 list the ABSPD and APD for each refrigerant. The ABSPD listed in Table 3 shows that the Shah correlation and Moser and Webb correlation tend to be the most accurate for R-134a, R-22 and R-410a with deviations ranging from 13% to 26%. R-407c has the highest ABSPD for each correlation with values ranging from 29% to 51%. Table 4 shows the APD for the four refrigerants. The Shah correlation and Moser and Webb correlation also tend to have the lowest ADP values with values under 11% for R-134a, R-22, and R-410a. The correlations on average all over predict the heat transfer coefficients for R-407c as would be expected since the mass transfer and temperature glide effects are not accounted for in these single component models.

Table 3: Average of absolute value of the percent deviations (ABSPD)

	Shah (%)	Caviellini (%)	Ackers (%)	Moser (%)
R-134a	12.91	16.14	30.29	15.36
R-22	25.98	32.43	24.48	21.37
R-410a	26.27	31.89	28.26	22.41
R-407c	33.74	50.66	34.3	28.96

Table 4: Average of percent deviations (APD)

	Shah (%)	Caviellini (%)	Ackers (%)	Moser (%)
R-134a	2.88	-8.09	27.72	10.72
R-22	-9.04	-20.54	12.43	1.56
R-410a	-4.83	-14.83	21.55	10.07
R-407c	-27.15	-46.54	-12.72	-18.96

Conclusion

The performances of refrigerants R-22, R-134a, R-410a, and R-407c were compared in a range of typical condenser tubes. Average and local heat transfer coefficients were measured over a range of mass fluxes, temperatures, and qualities. In all four test tubes, the average heat transfer coefficients were measured at a saturation temperature of 104 F (40 C) and over a mass flux range of 92,100 lb/ft²hr (125 kg/m² s) to 442,200 lb/ft² hr (600 kg/m²s). Local heat transfer coefficients were measured in the 3/8 inch (9.52 mm) outer diameter smooth tube and micro-fin tube. The local heat transfer coefficients were measured at an additional saturation temperature of 122 F over the same mass flux range.

A comparison of the performance of the different refrigerants reveals that R-134a has the highest performance, in both the smooth tube and the micro-fin tube, of all the refrigerants tested. R-22 and R-410a had similar performances which were slightly less than R-134a. In general, R-407c had the lowest performance of the refrigerants tested.

The performance benefit of the micro-fin tube is about the same for all the refrigerants tested. The micro-fin tube more than doubles the heat transfer coefficient during condensation for all refrigerants at the low mass fluxes but only increases the heat transfer coefficients by 50% at the higher mass fluxes. The local heat transfer coefficients showed that heat transfer coefficients decrease with increased saturation temperature. In addition, heat transfer coefficient dependence on quality is similar for the four refrigerants tested.

Acknowledgments

The authors would like to thank ASHRAE, for supporting this work with the ASHRAE New Investigator Award, and the companies that provided additional support: The Trane Company, Baltimore Aircoil, York International, Allied-Signal, Wolverine Tube Company, and Colmac Coil Company. In addition, the authors would like to thank members of the Project Monitoring Committee, Dr. Anthony Jakobi and Dr. Michael Ohadi.

Nomenclature

A=area (ft²)
C_p=Specific heat (BTU/(lb °F))
D_i=Test tube inner Diameter (ft)
D_o=Test tube outer diameter (ft)
EF=Heat Transfer Enhancement Factor
h=Heat transfer coefficient (BTU/(hr ft² °F))
i_{fg}=Enthalpy of vaporization (BTU/lb)
k=Thermoconductivity (BTU/(hr ft °F))
m=mass flow rate (lb/hr)
q=Heat transfer (BTU/hr)
q'=Heat flux (BTU/(hr ft²))
T=Temperature (°F)
U=Overall heat transfer coefficient (BTU/(hr ft² °F))
x=quality (%)
z=Length (ft)

Subscripts

a=Annulus
b=Boiler
r=Refrigerant
sat=Saturation
w=Water

References

- Akers, W.W., Deans, H.A., and Crosser, O.K., (1959). Condensing Heat Transfer within Horizontal Tubes. *Chemical Engineering Progress Symposium Series*. 55(29): 171-176.
- Bell, K. and Ghaly, M. (1972). An Approximate Generalized Design Method for Multicomponent/Partial Condensers. *Chemical Engineering progress Symposium Series*, **131** (69): 72-79.

- Briggs, D., and Young, E. (1969). Modified Wilson Plot Technique for Obtaining Heat Transfer Correlations for Shell and Tube Heat Exchangers. *Chemical Engineering Progress Symposium Series*. 65(92): 35-45.
- Cavallini, A, and Zecchin, R., (1974). A Dimensionless Correlation for Heat Transfer in Forced Convection Condensation. *Proc. Fifth International Heat Transfer Conference*. 3: 309-313.
- Chitti, M.S., and Anand, N.K., (1996) Condensation Heat Transfer Inside Smooth Horizontal Tubes for R-22 and R-32/125 Mixtures. *HVAC&R Research*. 2(1): 79-100.
- Dobson, M.K., and Chato, J.C., (1998) Condensation in Smooth Horizontal Tubes. *Journal of Heat Transfer*. 120: 193-213.
- Doerr, T., Eckels, S., and Pate, M. (1994). In-Tube Condensation Heat Transfer of Refrigerant Mixtures. *ASHRAE Transactions*, 101 (2): 547-557.
- Dunn, B. (1997) Heat Transfer Characteristics of Alternate Refrigerants Volume 2: Condenser Inside Tube. *EPRI Final Report TR-106016-V2*. EPRI, Palo Alto, CA.
- Gayet, Ph., Bontemps, A., and Marvillet, Ch. (1992). Condensation of Mixed Vapors of R-22 and R-1 14 Refrigerants Inside Horizontal Tubes. *Institution of Chemical Engineer's Symposium Series 2* (129): 1291-1300.
- Kedzierski, M.A, and Goncalves, J.M., (1997) Horizontal Convective Condensation of Alternative Refrigerants within a Micro-Fin Tube. *NISTIR 6095* U.S. Department of Commerce, Washington, D.C.
- Kline, S. and McClintock, F. (1953). Describing Uncertainties in Single-Sample Experiments. *Mechanical Engineering*, 75: 3-8.
- Manwell, S.P., Bergles, A.E. (1990) Gas-Liquid Flow Patterns in Refrigerant-Oil Mixtures *ASHRAE Transactions*, 96(2): 456-464.
- Mochizuki, S., Inoue, T., and Tominaga, M. (1988). Condensation Heat Transfer of Nonazeotropic Binary Mixtures (R-113 + R-11) in a Horizontal tube. *Transactions, JSME*, 54 (503B): 1796-1801.
- Moser, K.W., Webb, R.L., and Na, B. (1998). A New Equivalent Reynolds Number Model for Condensation in Smooth Tubes. *Journal of Heat Transfer* 120: 410-417.
- Nitheanandan, T., Soliman, H.M., and R.E. Chant. (1990). A Proposed Approach for Correlating Heat Transfer during Condensation Inside Tubes. *ASHRAE Transactions*, 96(1): 230-241.
- Ro, S., Jun, H., Chang, Y., and Shin, J. (1994). Condensation Heat Transfer of a Heat Pump System Using the Refrigerant Mixtures R-32/R-134a. *ASHRAE Transactions*, 100(2).
- Shah, M. M. (1979). A general correlation for heat transfer during film condensation inside pipes. *International Journal of Heat and Mass Transfer*, 22:547-556.
- Stoecker, W. and Kornota, E. (1985). Condensing Coefficients When Using Refrigerant Mixtures. *ASHRAE Transactions*, 91 (2B): 1351-1367.
- Tandon, T., Varma, H., and Gupta, C. (1985). An Experimental Investigation of Forced-Convection Condensation during Annular Flow Inside a Horizontal Tube. *ASHRAE Transactions*, 91 (1): 343-355.
- Thome, J.R., Favrat, D., and Nidegger, E. (1997). Heat Transfer and Pressure Drop in the Dryout Region of Intube Evaporation With Refrigerant / Lubricant Mixtures, *ASHRAE Final Report (800-RP)*, ASHRAE, Atlanta, GA.
- Wijaya H., and Spatzs, M. (1995). Two-Phase Flow Heat Transfer and Pressure Drop Characteristics of R-22 and R-32/125 *ASHRAE Transactions*, 101 (1): 1020-1027 .